International Journal of Computational Intelligence Systems (2023) 16:55
https://doi.org/10.1007/s44196-023-00239-0

RESEARCH ARTICLE

# Estimation for Human Motion Posture and Health Using Improved Deep Learning and Nano Biosensor

**Wenbo Xu**[1] · **Zhiqiang Zhu**[1]

Received: 8 February 2023 / Accepted: 6 April 2023


**Abstract**
To improve the technical level of human motion posture and health estimation, a human motion posture and health estimation algorithm based on Nano biosensor and improved deep learning is proposed. First, we use Nano biological acceleration sensor and Nano biological angular velocity sensor to obtain human motion posture and health data. Second, after the fusion processing of human motion posture and health data, we use the motion posture coordinate system conversion unit and the physiological information recognition unit to convert the coordinate system of human motion angular velocity and acceleration data and recognize the physiological information of blood pressure and heart rhythm. Finally, the convolution neural networks (CNN) in deep learning is improved to obtain the deformable CNN. The transformed angular velocity, physiological information recognition results and other human posture data are input into the deformable CNN, and the human posture estimation results are output. Experiments show that proposed algorithm can accurately obtain human posture data, can quickly and accurately estimate human posture, and has a good application effect. It has important application value in identity recognition and sports performance analysis.

**Keywords** Estimation · Human motion posture and health · Deep learning · Nano biosensor · Coordinate system conversion · Deformation bias

**Abbreviations**

| | |
|---|---|
| CNN | Convolutional neural networks |
| 3D | Three-dimensional |

## 1 Introduction

As one of the important technologies in computer vision, human posture estimation is a technology to obtain the current motion state of the target person through the image or the dynamic data of the target [1, 2]. It is widely used in games, identity recognition and sports performance analysis. At present, the biosensors used in the process of human posture estimation are difficult to capture the subtle posture changes of the human, so the Nano biosensor came into being. Nano biosensor is the fusion of nanotechnology and biosensor, using bio-specific recognition process to achieve the detection of sensor devices, bio-sensitive components including organisms, tissues, cells, organelles, cell membranes, enzymes, antibodies, nucleic acids and so on [3]. Its research involves many important fields such as biotechnology, information technology, nano science, interface science, and the integrated application of various advanced detection technologies such as light, sound, electricity and color, thus becoming the international research frontier and hotspot, compared with the general biosensor has a smaller size, faster, higher accuracy and reliability, free of labeling, good specificity, high efficiency and other advantages. The deformable convolutional neural networks (CNN) is an optimized form of convolutional neural network. Since the implementation of human posture estimation using CNN is complicated and the training time required is relatively long, the deformable convolutional neural network adds two modules of deformable convolution and deformable interest region pooling, which can be trained end-to-end by backward propagation algorithm to minimize the output error of the convolutional neural network and improve the training effect. Applying nano biosensor and deformable CNN to the

✉ Zhiqiang Zhu
zhuzhiqiang1960@126.com

Wenbo Xu
xu924276452@sina.com

[1] International College, Krirk University, Bangkhen, Bangkok 10220, Thailand

Published online: 17 April 2023

human pose estimation process can improve the estimation accuracy and speed [4].

At present, many experts and scholars in various fields have conducted in-depth research into human posture estimation and put forward the human posture estimation algorithm. For example, Hong et al. [5] proposed an augmented human posture recognition algorithm. In this method, a training classifier is used to amplify the linear mechanical features of human motion, and a linear dynamic model is constructed. The human posture estimation results are obtained using this model. However, the effect of this algorithm in dealing with the noise of the moving target image is not good, resulting in the deviation of the estimated human posture. Qiao et al. [6] used human posture activation map as input, and used three-dimensional (3D) CNN to obtain human posture estimation results by training human posture joint data. In the application of this method, the selection of neural network parameters is subjective, and the model iteration is easy to fall into extreme value, so the application effect is poor. Singu et al. [7] proposed a human posture estimation method based on a single RGB image. Human posture estimation consists of two steps, namely, human posture feature extraction and posture point cloud estimation. CNN is used to extract and train data features. CNN can learn posture and feature data to recognize human posture. Further, the obtained features and the estimated human posture are used to obtain the point cloud of human posture. However, in practical application, it is found that the algorithm has the problem of low accuracy of human posture data. Song et al. [8] proposed a human pose estimation algorithm based on 3D multi-view basketball data set. After the RGB basketball motion pictures in the three-dimensional multi-view basketball motion data set are passed through the semantic segmentation network, the picture containing the target object is obtained, and the picture is input into the constructed feature fusion network model. After feature extraction of the RGB image and the depth image respectively, the RGB feature, the local feature of the point cloud and the global feature are stitched and fused to form a feature vector, and the human posture is recognized by combining the feature vector. However, in practical application, it is found that this algorithm is difficult to effectively recognize human postures such as leg lifting and squatting. Sengupta et al. [9] proposed a real-time human skeleton posture estimation algorithm based on millimeter wave radar and CNN. The reflected radar point cloud is analyzed and projected on the range azimuth and range elevation planes, and a low size high-resolution radar image representation method is designed, that is, the normalized values of the distance, elevation/azimuth and the power level of the reflected signal are allocated to the RGB channel. The algorithm uses a forked CNN structure and radar image representation to predict the real posture of bone joints in three-dimensional space, and realizes human posture estimation according to the prediction results. However, this algorithm has the problem of large estimation of human posture deviation.

To effectively address the problems of the above algorithms, a human posture estimation model is built through improved deep learning, and then the basic data of human motion posture and health is obtained using Nano biosensor acceleration sensors, angular velocity sensors in the data perception layer. The ability of human posture data can quickly and accurately estimate human posture. The main contributions of this paper are as follows: (1) The use of Nano biosensor to acquire human motion posture and health data solves the difficulty of traditional sensors to accurately capture subtle posture changes, and ensures the accuracy and speed of data collection results. (2) In this paper, the modified CNN model is improved and applied to human posture estimation, which solves the problem that the output result is not accurate if the parameter selection is unqualified. (3) The results using different data sets show that the proposed human posture estimation algorithm can effectively estimate the posture of human body such as leg lifting and squatting, and the application effect is good.

## 2 Methodology

### 2.1 Technical Framework of Human Pose Estimation Algorithm

The technical architecture of the human posture estimation algorithm is designed according to the layered idea, as shown in Fig. 1.

The technical architecture of human posture estimation algorithm is composed of data perception layer, service layer and an interaction layer. The basic data of human motion posture and health is obtained using nano-biological acceleration sensor, and angular velocity sensor in the data sensing layer. The nano-biological acceleration sensor is a kind of sensor that can measure acceleration. After the inertial force on the mass is measured, the acceleration value of the human is obtained using Newton's second law of motion; the physical quantity measured by the angular velocity sensor is the rotational angular velocity when the human deflects and tilts; blood pressure sensor can ensure the smooth progress of accurate continuous measurement of human blood pressure. All sensors are arranged at appropriate postures to collect basic data on human motion posture and health. On this basis, the wireless sensor network is used to transmit all data to the data integration unit in the service layer. The

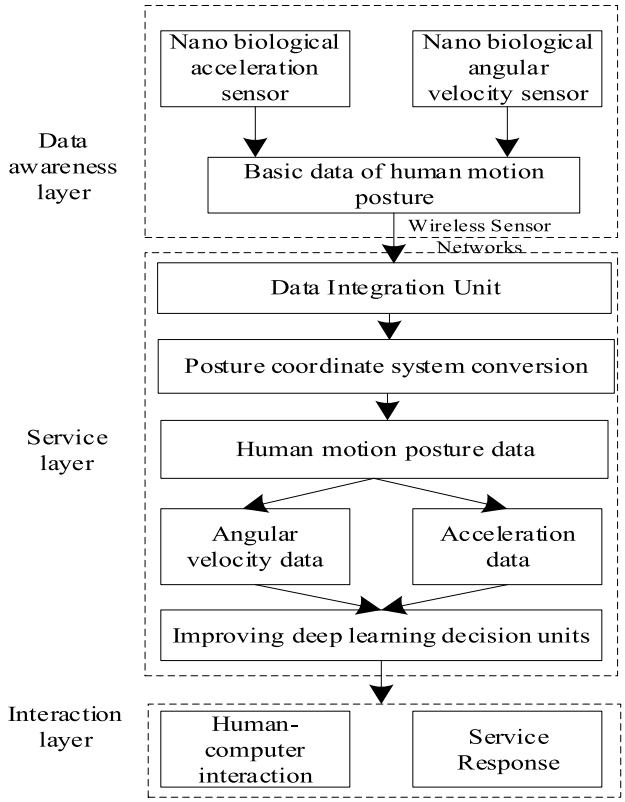


**Fig. 1** Technical architecture of human pose estimation algorithm

protocol used in the wireless sensing network is a clustering-based routing protocol. The data integration unit converts the angular velocity and acceleration data in the basic human motion posture data to obtain the human motion posture data in the motion posture coordinate system.

Human motion posture and health data and physiological information recognition results are input. The deformed CNN model in the improved deep learning decision unit is used to estimate the human motion posture and health, and the estimation results are transmitted to the interaction layer. The human–machine interaction and service response unit in the interaction layer are used to present the human motion posture and health estimation results to the user. The structure of the Nano biosensor network is shown in Fig. 2.

According to the data in Fig. 2. In this paper, the nano-bio angular velocity sensor as well as the nano-bio acceleration sensor are installed in the monitoring area. The measurement range of the nano angular velocity sensor is ± 7200°, the sensitivity is mV/°, and the sampling frequency is 0–40 Hz, and the measurement range of the nano angular velocity sensor is ± 8 g, the sensitivity is 200 pm/g, and the sampling frequency is 0–40 Hz. After the Nano biological sensor obtains all the data in the process of human motion, it will send the data to the base station and transmit it to the task management node through the internet and satellite, so that it can be called at any time, ensuring the accuracy and efficiency of data collection.

## 2.2 Transformation of Motion Posture Coordinate System

After obtaining the angular velocity and acceleration of the human body in the process of motion using the nano-biological angular velocity sensor and the nano-biological

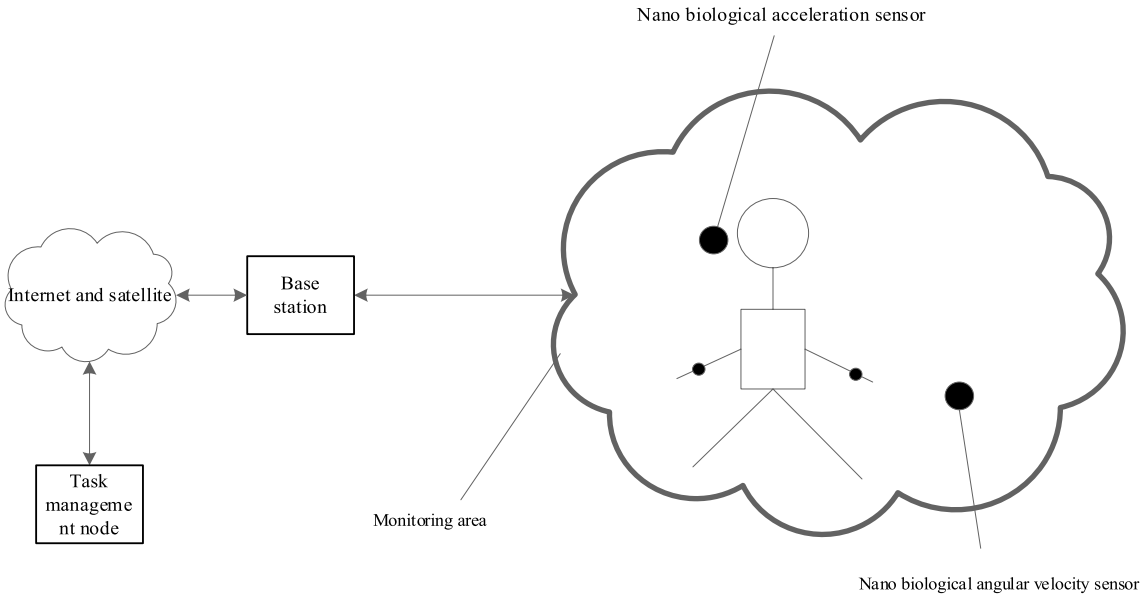


**Fig. 2** Structure of nano biosensor network

acceleration sensor, it is necessary to convert the human body coordinate system and the geographical coordinate system where the angular velocity and acceleration are located to ensure the uniformity of the data [10, 11]. Here, the coordinate system in which the angular velocity and acceleration of Euler angle are located is used for conversion. The detailed process is as follows:

Let $OX_0Y_0Z_0$ be human body coordinate system of angular velocity and acceleration. After the Euler angle is converted twice, the geographic coordinate system $OXYZ$ of angular velocity and acceleration is obtained. The expression formula for converting human body coordinate system and geographical coordinate system is as follows:

$$\begin{aligned} &OX_0Y_0Z_0 \\ &\downarrow X_0/\theta_1 \\ &OX_1Y_1Z_1 \\ &\downarrow Y_1/\theta_2 \\ &OX_2Y_2Z_2 \\ &\downarrow Z_2/\theta_3 \\ &OXYZ \end{aligned} \tag{1}$$

where $OX_1Y_1Z_1$ and $OX_2Y_2Z_2$ refer to the first and second transition coordinate systems during coordinate conversion, respectively; $\theta_1$, $\theta_2$ and $\theta_3$ refer to the rotation angle during coordinate system transformation, which is the Euler angle.

The angular relationship between the coordinate systems $OX_0Y_0Z_0$ and $OXYZ$ is described by converting the Euler angle into the coordinate system of angular velocity and acceleration. Then the direction cosine matrix formula of the coordinate system $OX_0Y_0Z_0$ and the transition coordinate system at the first conversion is

$$G_0^1 = \begin{bmatrix} 1 & 0 & 0 \\ 0 & \cos\theta_1 & \sin\theta_1 \\ 0 & -\sin\theta_1 & \cos\theta_1 \end{bmatrix} \times \varepsilon, \tag{2}$$

where $G_0^1$ refers to the direction cosine matrix at the first conversion of coordinate system $OX_0Y_0Z_0$; $\varepsilon$ is the adjustment factor.

The direction cosine matrix $G_1^2$ formula of the coordinate system $OX_0Y_0Z_0$ and the transition coordinate system during the second conversion

$$G_1^2 = \begin{bmatrix} \cos\beta & 0 & -\sin\theta \\ 0 & 1 & 0 \\ \sin\theta_2 & 0 & \cos\theta_2 \end{bmatrix} \times \varepsilon, \tag{3}$$

where $\beta$ indicates the posture angle.

The expression formula of the direction cosine matrix between the transition coordinate system and the geographical coordinate system during the second conversion is as follows:

$$G_1^2 = \begin{bmatrix} \cos\theta_3 & \sin\theta_3 & 0 \\ -\sin\theta_3 & \cos\theta_3 & 0 \\ 0 & 0 & 1 \end{bmatrix} \times \varepsilon. \tag{4}$$

According to the results of formulas (2)–(4), the conversion relationship between the angular velocity and acceleration coordinate system and the geographic coordinate system is obtained

$$\begin{bmatrix} x_0 \\ y_0 \\ x_0 \end{bmatrix} = G \begin{bmatrix} x \\ y \\ z \end{bmatrix} \times \varepsilon, \tag{5}$$

where $x$, $y$ and $z$ refer to the three directions of the coordinate system, respectively; $G$ refers to the direction cosine matrix of coordinate system transformation. And $G = G_2^3 G_1^2 G_0^1$.

The transformation between the coordinate system of angular velocity and acceleration and the geographical coordinate system can be completed using formula (5).

### 2.3 Human Posture Estimation Model Based on Improved Deep Learning

CNN is the most widely used in deep learning. If the parameters of CNN are unqualified, the output results will be inaccurate. Therefore, a new deformable CNN is designed to improve the deep learning method.

The deformable CNN is derived from the CNN. The geometric deformation ability in the CNN model is added to make the output result of the CNN more accurate [12]. The angular velocity and acceleration coordinate conversion results are input into the front-end network of the deformed CNN model. After deformation bias processing and deformation convolution operation, the angular velocity, acceleration and other data are input into the self-inference network, and then a relay supervision module is constructed [13, 14]. The self-inference network is controlled by the module to output the human posture estimation results.

(1) Deformation bias of deformed CNN.

Let $J_{\text{out}}$ be human posture features of the front-end network output of the deformable CNN. The expression formula is as follows:

$$J_{\text{out}} = \text{Head}(\text{data}), \tag{6}$$

where Head(·) refers to the mapping relation of front end of deformable CNN; data refers to the angular velocity, acceleration and biological data of human body input into deformation CNN.

Geometric deformation processing is performed on the angular velocity, acceleration and human biological data in the front-end network of the deformation CNN, and the

deformation bias is calculated first [15]. Set $y$ as human posture features of the front-end network output of the deformable CNN. The feature point on the human posture feature is expressed by $y(O_0)$. The expression formula of the feature point is

$$y(O_0) = \sum_{p_n \in \hbar} w(o_n) \times \sum_{p_n \in \hbar} \left[ \left( xo_0 + xo_n \right) \right], \tag{7}$$

where $\hbar$ refers to the convolution kernel sampling grid; $o_n$ denotes the position point corresponding to convolution kernel sampling network; $O_0$ refers to the feature of human posture; $(xo_0 + xo_n)$ refers to the weighted sum of human posture features and relative positions of convolution kernel;$w(o_n)$ stands for the weight of human posture feature.

Set there are $N$ relative position points in the deformed convolution mesh, the bias of the convolution kernel requires $N \times 2$ bias outputs. When the human posture features are input into the deformation convolution kernel, the input channel and output channel are respectively $C_{\text{in}}$ and $C_{\text{out}}$, respectively. Then the bias value of the front-end network of the deformed CNN is $H \times W \times C_{\text{in}} \times C_{\text{out}}$, in which $W$ and $H$ refer to the width and height values of human posture features.

Based on the bias value of the front-end network of the deformed CNN, the front-end network of the deformed CNN is deformed, as shown in Fig. 3.

(2) Deformation convolution operation of deformation CNN.

After the basic data of human posture angular velocity and acceleration are input in the deformation CNN, the bias feature data is obtained through bias processing, and then the deformation convolution kernel operation is performed on the bias feature data, and the fused human posture data is obtained through back propagation[16, 17]. Then the self-inference network of the deformable CNN is constructed.

Set $ZF_0$ as the output value of self-inference network of CNN. The expression formula is as follows:

$$ZF_0 = \text{SINet}_0(J_{\text{out}}), \tag{8}$$

where $\text{SINet}_0(\cdot)$ represents the initial mapping relationship of the self-inference network.

When the series of self-inference networks is $i$, its output numerical expression formula is as follows:

$$ZF_i = \text{SINet}_i\left( \sum_{j=0,\ldots,i-1} IS_j \right) + \text{SINet}_i(J_{\text{out}}), \tag{9}$$

where $IS_j$ represents the output value of the relay supervision module. $j$ represents the number of relay supervision modules.

Set $IS_i$ as the integrated human posture feature data output from the monitoring module of level $i$, $\varphi_i$ refers to the estimated thermal data of relay supervision module. Then, the relationship between $IS_i$ and $\varphi_i$ is expressed as:

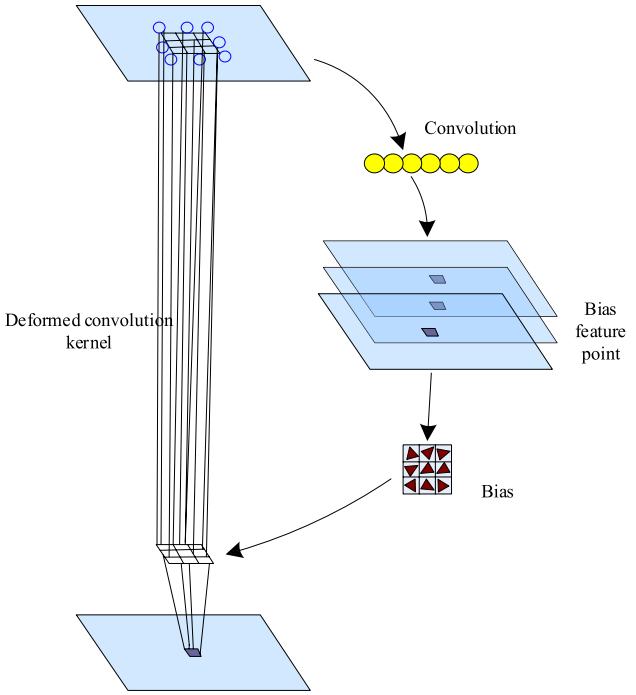


**Fig. 3** Deformation process of deformation CNN

$$IS_i, \varphi_i = InS_i(ZF_i) \tag{10}$$

where $InS_i(\cdot)$ represents the mapping relationship of the level $i$ relay supervision module.

The expression formula of $\varphi_i$ is as follows:

$$\varphi_N = \text{Fout}(ZF_N), \tag{11}$$

where $\text{Fout}(\cdot)$ refers to the mapping relation of final output results of deformed convolution network model; $N$ refers to the number of relay supervision modules.

(3) Optimization of deformed CNN based on non-maximal value suppression.

Since the modified deformable CNN is easy to fall into the extreme value in the iterative process [18, 19], the parameterized posture non-maximum suppression method [20] is used to improve it.

Set $d(U_i, U_j|\wedge)$ as the measurement function of human posture distance. This function is used to describe the similarity between human postures [21]. Then, the redundant posture elimination rule of $d(U_i, U_j|\wedge)$ is as follows

$$d(U_i, U_j|\wedge, \eta) = \left[ d(U_i, U_j|\wedge, \lambda) \times \delta \le \eta \right], \tag{12}$$

where $U_i$ and $U_j$ refer to the $i$ and $i$ estimation results of human motion posture and health; $d(\cdot)$ refers to the function,

whose parameter is $\wedge$; $\eta$ and $\lambda$ are the threshold and variable parameter; $\delta$ is the constant number.

Set $B_i$ as the target framework of human posture $U_i$, and the matching function expression formula of the target box is

$$K_{\text{sim}}(U_i, U_j|\sigma_1) = \sum_n \tanh(c_i^n/\zeta_1) \times \tanh(c_j^n/\zeta_1), \tag{13}$$

where $\zeta_1$ refers to the matching function parameter; $\sigma_1$ and $c_j$ refer to the credibility of human motion posture and health $i$ and $j$; $n$ refers to the number of human motion posture and health.

Set the key feature distance of motion posture as $H_{\text{sim}}(U_i, U_j|\zeta_2)$, and its expression formula is

$$H_{\text{sim}}(U_i, U_j|\zeta_2) = \sum_n \exp\left(-\frac{k_i^n}{\zeta_2}\right) - \sum_n \exp\left(-\frac{k_j^n}{\zeta_2}\right), \tag{14}$$

where $\zeta_2$ refers to the distance function parameters of key features of motion posture; $k_i^n$ and $k_j^n$ refer to the key points of the $i$ and $j$ human body motion posture.

After formula (13) is combined with formula (14), the final human body estimated posture distance measurement function is obtained, and the expression formula is as follows:

$$d(U_i, U_j|\wedge) = \lambda \times \left[K_{\text{sim}}(U_i, U_j|\zeta_1) + H_{\text{sim}}(U_i, U_j|\zeta_2)\right]. \tag{15}$$

After formula (15) is introduced into formula (8), the deformed CNN can avoid falling into the iterative extremum and realize human posture estimation. The human motion posture data are input into the optimized deformed CNN to obtain the relevant human posture estimation, which guarantees the maximum estimation accuracy and efficiency with good practical application-type results.

## 3 Experimental Results and Analysis

### 3.1 Data Sets

COCO dataset: like the ImageNet competition, it is regarded as one of the most concerned and authoritative competitions in the field of computer vision. After the suspension of the ImageNet competition, the COCO competition has become the most authoritative and important benchmark in the field of target recognition and detection. It is also the only competition in the world that can bring together Google, Microsoft, Facebook and many top universities and excellent innovative enterprises at home and abroad. The COCO dataset contains 200,000 images and more than 500,000 target annotations in 80 categories. It is a widely publicized target detection database, with an average number of targets per image of 7.2.

SURREAL dataset: The SURREAL dataset is a large-scale artificial gesture recognition dataset. For RGB video, it annotates a variety of states: depth information, body parts, optical flow, 3D gestures, etc. These images are the real rendering of people with great changes in shape, texture, viewpoint and posture, and contain 6 million frames of synthetic human body data.

The data in the two data sets were integrated, and 5000 images were randomly selected for experimental testing. The experimental data size was 23.56 G. In 5000 experimental images, 80% of the train sets and 20% were test sets. The data volume of the two sets is 18.71 G and 4.85 G, and the maximum number of features is 7. The data in the test set is input into the simulation software for trial operation. After several tests, the optimal experimental parameters were obtained, and the parameters were applied to the subsequent experiments, and the subsequent tests were completed using the data in the experimental set.

### 3.2 Evaluation Metrics

Based on the COCO dataset and the SURREAL data set, the motion posture is estimated using the algorithm in this paper, and the practical application effect of the algorithm is verified. At the same time, the algorithm in Variant grassmann manifolds [5], the algorithm in Lam-2srn [6], the algorithm in PCHP [7], the algorithm in HPRE [8], and the algorithm in mm-Pose [9] were used to experiment.

The human posture data acquisition accuracy is taken as an experimental index, the higher the value, the higher the accuracy of the obtained human posture data. The calculation formula of indicators is as follows:

$$A = \frac{a_2}{a_1} \times 100\%, \tag{16}$$

where $a_1$ is the amount of human posture data used in the experiment, and $a_2$ is to the amount of human posture data accurately collected by different algorithms.

Fitting test: different methods have been used for fitting tests. The closer the fitting curve is to the feature point of human posture data, the higher the fitting degree and the better the practical application effect.

The calculation formula of motion posture estimation accuracy is as follows:

$$E = \frac{D_K}{D_Z} \times 100\%, \tag{17}$$

where $D_K$ represents the sample size of human posture correctly estimated by different methods.$D_Z$ represents the total number of samples.

Human posture coincidence degree: this index refers to the coincidence degree between the human posture

estimation result and the actual result under the number of jumps of the target. The calculation formula of this index is

$$W = |w_1 - w_2|, \tag{18}$$

where $w_1$ represents the estimation result of human posture. $w_2$ is the actual result.

The estimation efficiency of this algorithm is tested when the number of estimated motion postures is different. The calculation formula of indicators is as follows:

$$T = \sum_{i=1}^{n} t_i, \tag{19}$$

where $t_i$ represents the time consumption of the $i$th human posture estimation step.$n$ represents the total steps of human posture estimation.

### 3.3 Results and Discussion

The angular velocity, acceleration, blood pressure and other data obtained by the Nano biosensor are the basis of human posture recognition. Experimental data acquisition accuracy verifies the ability of this paper's algorithm to acquire human posture data using nano biosensor, which is the average accuracy of all nano biosensor, as shown in Table 1.

According to the data in Table 1. The accuracy of human posture data acquisition of proposed algorithm shows a fluctuating trend, and reaches the maximum value of 99.6% at the 40$^{th}$ time. And the average accuracy of the human posture data acquisition of this algorithm is 98.1%, which is 11.5%, 5.2%, 1.5%, 21.5% and 7.9% higher than the algorithms in Variant Grassmann manifolds [5], Lam-2srn [6], PCHP [7], HPRE [8] and mm-Pose [9], respectively. The reason is that the algorithm uses nano- biosensors to acquire human posture data. Therefore, it ensures the accuracy and quality of data acquisition, which proves that the proposed algorithm has a strong ability to acquire human posture data.

Taking the fitting degree as the measurement index, the fitting degree of different algorithms is tested, and the results are shown in Fig. 4. It can be seen in Fig. 4.The

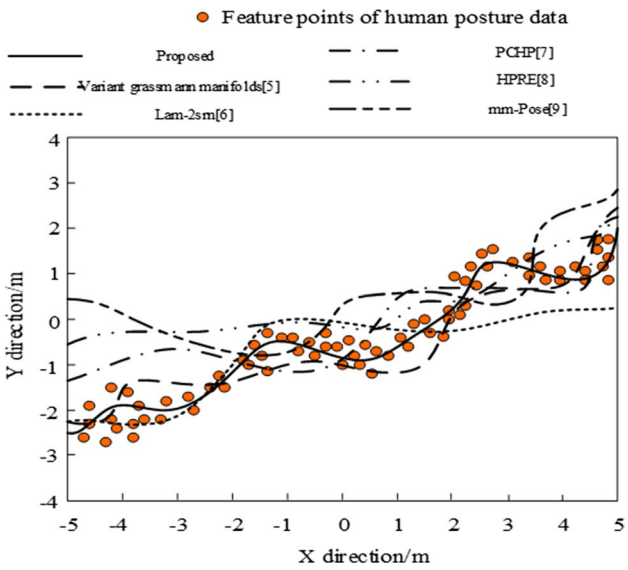


**Fig. 4** Comparison results of fitting

fitting curve of the algorithm in Variant Grassmann manifolds [5] is close to the feature points of human posture data, but there is a large deviation in some areas. The fitting curve of the algorithm in Lam-2srn [6] coincides with the feature points of human posture data in the interval of $[-5, -1]$ in the X direction, but there is a large distance from the feature points of human posture data. The algorithm in PCHP [7] is far from the feature point position of human posture data, while the algorithm in HPRE [8] has a large deviation from the feature point position of human posture data and poor fitting. The algorithm in mm-Pose [9] is far from the feature points of human posture data, while the trend of the fitting curve of the proposed algorithm when estimating human posture is completely the same as the distribution trend of the feature points of human posture data. Moreover, the fitting curve of the proposed algorithm is close to the position of the feature points of the human posture data, which indicates that there is no fitting phenomenon when estimating the human

**Table 1** Data acquisition accuracy (%)

| Number of experiments | Variant Grassmann manifolds [5] | Lam-2srn [6] | PCHP [7] | HPRE [8] | mm-Pose [9] | Proposed |
|---|---|---|---|---|---|---|
| 10 | 85.6 | 93.4 | 75.6 | 74.5 | 90.2 | 96.8 |
| 20 | 84.7 | 94.7 | 74.1 | 86.3 | 91.4 | 97.9 |
| 30 | 85.9 | 82.6 | 72.3 | 87.4 | 86.3 | 98.5 |
| 40 | 84.2 | 93.5 | 75.9 | 84.2 | 89.3 | 99.6 |
| 50 | 93.5 | 97.4 | 76.3 | 85.1 | 86.4 | 98.7 |
| 60 | 85.6 | 95.6 | 85.6 | 86.3 | 97.7 | 96.9 |
| Average value | 86.6 | 92.9 | 76.6 | 84.0 | 90.2 | 98.1 |

posture, and the output human posture estimation result is more accurate.

Table 2 shows the comparison results of motion posture estimation accuracy. The accuracy of motion posture estimation of this algorithm shows a fluctuating trend. When the number of experiments reaches 50, the maximum accuracy of motion posture estimation reaches 99.1%. The average estimation accuracy of this algorithm is 98.1%, which is 21.4%, 13.7%, 12.3%, 12.8% and 13% higher than the algorithms in Variant Grassmann manifolds [5], Lam-2srn [6], PCHP [7], HPRE [8] and mm-Pose [9], respectively. It shows that the proposed algorithm can effectively estimate human motion posture and health, and has certain application effect.

Taking the coincidence degree of human posture recognition as a measurement index, the proposed algorithm is used to estimate the posture. At the same time, the algorithm in Variant grassmann manifolds [5], the algorithm in Lam-2srn [6], the algorithm in PCHP [7], the algorithm in HPRE [8], and the algorithm in mm-Pose [9] are also used to experiment, as shown in Fig. 5.

According to the data in Fig. 5.The coincidence degree of the six human posture estimation methods for human posture recognition decreases with the increase of the number of jumps of the estimated target, and the decrease of the coincidence degree of the human posture estimated by the proposed algorithm, the algorithm in Lam-2srn [6] and the algorithm in HPRE [8] is similar. However, among the six methods, the proposed algorithm has the highest accuracy. When the estimated number of jumps of the target is 100 times, the coincidence degree of the target posture estimated by the proposed algorithm is about 98.5%, which is 3.5%, 1.2%, 5.1%, 1.9% and 6.1% higher than the algorithms in Variant Grassmann manifolds [5], Lam-2srn [6], PCHP [7], HPRE [8] and mm-Pose [9], respectively, indicating that the coincidence degree of the proposed algorithm is higher.

The estimation efficiency is taken as the performance index of the proposed algorithm, and it is tested under the different number of estimated motion postures. The results are shown in Fig. 6.

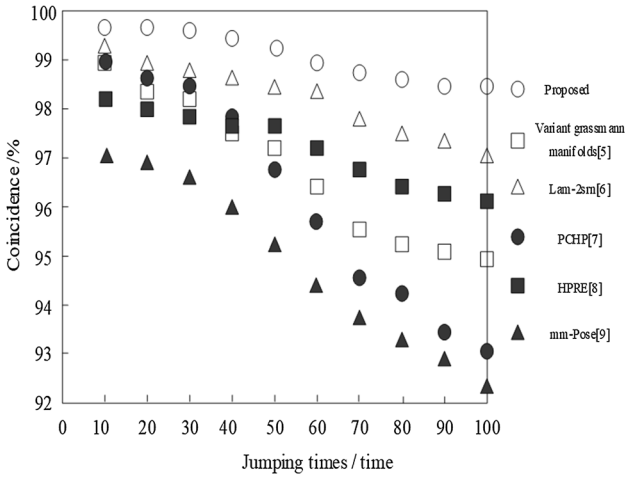


**Fig. 5** Comparison results of estimated human posture coincidence

It can be seen in Fig. 6. The time efficiency of the six algorithms for estimating human posture is inversely proportional to the amount of human posture data. Before the amount of human posture data is 2300, the time efficiency of this algorithm for estimating human posture shows a small upward trend. When the amount of human posture data exceeds 2300, the estimated human posture time of the proposed algorithm presents a large upward trend, lasting to 3000. When the amount of human posture data is between 3000 and 4800, the human posture estimation time presents a balanced state. When the amount of human posture data is between 4800 and 5600, the human posture estimation time shows a rapid upward trend. When the amount of human posture data is 10,000, the maximum time of human posture estimated by the proposed algorithm is only about 3.5 s, which is 7.8 s, 5.7 s, 4 s, 5.9 s and 8 s lower than the algorithms in Variant grassmann manifolds [5], Lam-2srn [6], PCHP [7], HPRE [8] and mm-Pose [9], respectively. The results show that the proposed algorithm has a short time to estimate human posture and is less affected by the amount of human posture data.

**Table 2** Comparison results of motion attitude estimation accuracy (%)

| Number of experiments | Variant Grassmann manifolds [5] | Lam-2srn [6] | PCHP [7] | HPRE [8] | mm-Pose [9] | Proposed |
|---|---|---|---|---|---|---|
| 10 | 79.6 | 86.3 | 89.6 | 85.1 | 86.3 | 98.7 |
| 20 | 75.8 | 87.4 | 95.3 | 87.4 | 85.5 | 96.9 |
| 30 | 74.3 | 84.6 | 82.3 | 85.3 | 87.1 | 98.2 |
| 40 | 74.6 | 85.3 | 82.5 | 90.3 | 83.6 | 96.8 |
| 50 | 75.6 | 87.4 | 86.4 | 87.4 | 81.4 | 99.1 |
| 60 | 80.3 | 75.6 | 78.6 | 76.3 | 86.9 | 98.6 |
| Average value | 76.7 | 84.4 | 85.8 | 85.3 | 85.1 | 98.1 |

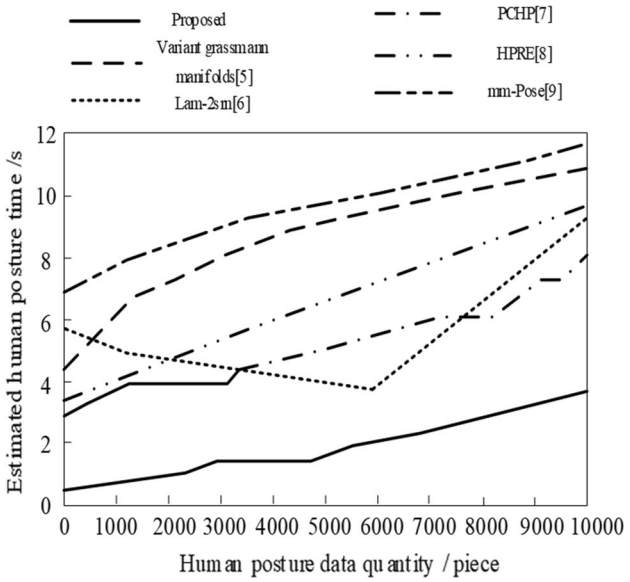


**Fig. 6** Comparison results of time efficiency for estimating human posture

## 4 Conclusions

The paper applies Nano biosensor to the process of collecting human body estimation data. Nano biosensor has the characteristics of accurate and portable data acquisition. The experimental verification shows that the average accuracy of the human posture and health data acquisition of the proposed algorithm is 98.1%, and the trend of the fitting curve when estimating the human posture and health is the same as the distribution trend of the characteristic points of the human posture and health data, the average accuracy of the estimation is 98.1%, the coincidence of the estimated target posture is about 98.5%, and the maximum human posture and health estimation time is only about 3.5 s. Although the proposed algorithm has a strong ability in estimating human posture, there are still some technical defects in this paper. For example, the proposed algorithm does not de-noise the human posture and health data obtained by the Nano biosensor. Although the human posture and health data obtained by the Nano biosensor is relatively accurate, there are still different degrees of interference noise in the data, which affects the results of estimating human posture and health. Therefore, more research will be conducted on this in the future to solve the impact of noise on the estimation results.

**Author Contributions** Conceptualization and methodology: WX. Data curation, validation, writing—review and editing: ZZ.

**Funding** The authors received no funding for this study.

**Data Availability Statement** The data used to support the findings of this study are included in the article.

## Declarations

**Conflict of interest** The authors declare that they have no competing interests.



## References

1. Toshpulatov, M., Lee, W., Lee, S., Rou, D., Sari, A.H.: Human pose, hand and mesh estimation using deep learning: a survey. J. Supercomput. **78**(6), 7616–7654 (2022)
2. Vargas, J., Pedrycz, W., Hemerly, E.M.: Improved learning algorithm for two-layer neural networks for identification of nonlinear systems. Neurocomputing **329**, 86–96 (2019)
3. Samarthrao, K.V., Rohokale, V.M.: Enhancement of email spam detection using improved deep learning algorithms for cyber security. J. Comput. Secur. **30**(2), 231–264 (2022)
4. Sengupta, A., Jin, F., Zhang, R., Cao, S.: mm-Pose: real-time human skeletal posture estimation using mmWave radars and CNNs. IEEE Sens. J. **20**(17), 10032–10044 (2020)
5. Hong, J., Li, Y., Chen, H.: Variant Grassmann manifolds: a representation augmentation method for action recognition. ACM Trans. Knowl. Discov. Data **13**(2), 1–23 (2019)
6. Qiao, Y., Cui, W., Shi, T.: Lam-2srn: a method which can enhance local features and detect moving objects for action recognition. IEEE Access **8**, 192703–192712 (2020)
7. Singu, P., Lakshmi, V., Raajan, N.R.: Point cloud human posture estimation using single RGB image. Mater. Today Proc. **33**(7), 3907–3911 (2020)
8. Song, X., Fan, L.: Human posture recognition and estimation method based on 3D multiview basketball sports dataset. Complexity **15**(1), 1–10 (2021)
9. Sengupta, A., Jin, F., Zhang, R., et al.: mm-Pose: real-time human skeletal posture estimation using mmWave radars and CNNs. IEEE Sens. J. **20**(17), 10032–10044 (2020)
10. Wang, C., Zheng, J., Bo, J., Liu, H., Shi, Y.: Deep neural network-aided coherent integration method for maneuvering target detection. Signal Process. **182**(9), 107966 (2021)
11. Lyu, P., Wei, G., Cui, W.: Short-range multi-target motion parameter estimation method based on hough transform. Chin. J. Electron. **28**(02), 125–129 (2019)
12. Jung, H., Ju, J., Hwang, W., Kim, J.: Refining background subtraction using consistent motion detection in adverse weather. J. Electron. Imaging **28**(2), 020501 (2019)
13. Jiang, S., Qi, H., Zhang, J., Zhang, S., Ming, D.: A pilot study on falling-risk detection method based on postural perturbation evoked potential features. Sensors **19**(24), 5554 (2019)

14. Han, K., Yang, Q., Huang, Z.: A two-stage fall recognition algorithm based on human posture features. Sensors **20**(23), 6966 (2020)
15. Gao, X.S., Yang, T., Peng, J.M.: Logic-enhanced adaptive network-based fuzzy classifier for fall recognition in rehabilitation. IEEE Access **8**, 57105–57113 (2020)
16. Ji, Y., Zhan, Y., Yang, Y., Xu, X., Shen, H.T.: A context knowledge map guided coarse-to-fine action recognition. IEEE Trans. Image Process. **29**, 2742–2752 (2020)
17. Tu, Z., Li, H., Zhang, D., Dauwels, J., Li, B., Yuan, J.: Action-stage emphasized spatiotemporal VLAD for video action recognition. IEEE Trans. Image Process. **28**(6), 2799–2812 (2019)
18. Xing, M., Feng, Z., Su, Y., Peng, W., Zhang, J.: Ventral & dorsal stream theory based zero-shot action recognition. Pattern Recognit. **116**(5), 107953 (2021)
19. Xia, Z.H., Xing, J.M., Li, X.F.: Gesture tracking and recognition algorithm for dynamic human motion using multimodal deep learning. Secur. Commun. Netw. **2022**, 1–11 (2022)
20. Zhang, S.W., Deng, C.H., Zhang, J.W.: Application of anisotropic non-maximum suppression in industrial target detection. J. Comput. Appl. **7**, 2210–2218 (2022)
21. Majd, M., Safabakhsh, R.: A motion-aware ConvLSTM network for action recognition. Appl. Intell. **49**(7), 2515–2521 (2019)